Electrically Multi-layered Small Implantable Antenna for Medical Devices: Design and Characterization

Ashraf Sayed Abdel Halim

Department of Communication, Faculty of Engineering, Canadian International Collage (CIC), Egypt.
ashraf_sayed@cic-cairo.com

Abstract: This study illustrates the design method for the implementation of electrically multi-layered small implantable antenna for biotelemetry processes. The suggested antenna consists of three layers arranged in a stack, pressed on high permissively, grounded substratum. The deepest layer of the antenna above the ground flat surface contains a meandered construction with a precisely placed T-shaped aperture. The intermediate segment consists of2 U- contoured radiators and an M- contoured metallic part is moreover added on the highest segment for additional enhancement of the radiation efficacy of the antenna. These three stacked layers form a symmetrical closed loop structure resonating on its fundamental resonant design, at 403 MHz, for the Medical Implant Communication Service (MICS) band. A shifted higher system procedure of the similar enclosed loop design, along the negative currents on ground level allowing broad band process, at 2.45 GHz, for the industrialized, scientific, and medical (ISM) band. To clarify the resistance accompanying implanting of an antenna in human body that mostly resulting in detuning and impedance mismatch, the antennas most relevant radiating sections were completely investigated. A fully parametrized solution is suggested that makes the antenna a good candidate for an apparatus, implanted at many separate areas of the human being with reasonably specific electrical characteristics with consequently peculiar detuning influence. Toward additional analysis, the particle swarm algorithm was fulfilled to improve the antennas practice during working within a compressed, 23x23x5mm^{3}blockade of human skin, equivalent phantom. The simulated operation of the suggested prototype antenna, reveals that it can be employed, toward whether in-vitro or in-vivo processes. Any wireless communication between implantable antenna and an external outside-body antenna suffers significant link loss because of the lossy character of live human tissues. This link deterioration is normally unreliable and varies for different sectors of the human body. To investigate an implantable connection scenario, complete setup is broadly simulated utilizing a full wave electromagnetic simulator. This simulation requires human body phantoms carrying electrical characteristics as permittivity and mass conductivity, or still bulk density similar to that of human tissues. It has been observed that geometry of these phantoms is frequently chosen as simple as feasible to minimize the needed computational means and the overall time for the fulfillment of the simulation. It is problematic to expect how much inaccuracy is predicted when realistic phantom is replaced by geometrically simpler phantom. This work focuses on superiority of applying realistic human body phantoms over geometrically simple body phantoms for entire body transmission simulation. To test this relationship, an implantable antenna, located inside a human stomach prototype, is established to connect with an outside body antenna at MICS b and Maintaining the separation among implantable antenna and outside-body antenna fixed, the realistic human body phantom is then substituted by 2varieties of geometrically simpler phantoms with disparate complexity. Results in the form of calculated s-parameters and phantom complexity metrics are further investigated to conclude the study.

1. Introduction

Antennas are fundamental principle of implantable medical materials used in increasing number of operations for checking physiological criteria and wirelessly connecting with other in-body or off-body devices [1].

This work discusses the design method towards the implementation of a compact, stacked, implantable antenna for biotelemetry applications. Planning an implant able antenna is difficult mission due to some factors. First and most prominent threat is the detuning factor and impedance mismatching that develops mean while the antenna is situated interior human body. This is because of excessive water content and strong conductive human tissues. Furthermore detuning and mismatching are typically uncertain and differ from tissue to tissue as various tissues have diverse electrical characteristics. The second dominant obstacle which develops during planning implantable antenna is its size. Considering, MICS band at 403 MHz is selected for implantable materials for inside-body equipment communication, the antenna

activehole region at this frequency is somewhat large. But, the demandis that the antenna interspersed with the implantable device, with power unit, must be small enough, as the equipment is proposed to be implanted in the human body. A considerable work has already been carried out where various antenna model topologies have been suggested by investigators [2].

To investigate the act of an antenna inside the body, simulations are frequently adoptedinside simple layered phantoms [3, 4], or interior of realistic body phantoms [5, 6]. Electrical characteristics of these phantoms are planne dutilizing Cole-Cole design [4, 7] or multi-pole Debye design [8]. In addition some investigators [7, 9, 5] examined the electrical characteristics of human tissues utilizing dielectric probe kit or impedance analyzer and then utilized these characteristics in simulations to investigate the performance of their suggested solution. In order to accomplish compactness, investigators have test edvarious techniques and many patterns of antennas, like spiral [4, 10, 11], meandered patch [6, 7, 9, 10, 11], folded square IFA [12], 2D and 3D spherical [13, 10] and multilayered [14] shapes. All these methods decrease the antenna size by rising the length of the current flow direction on the corresponding plane (meandered and spiral) or in all 3 dimensions. In addition, a shortening pin between ground and patch may additionally effectually decrease the needed physical parameters of animplan table antenna [15] and has been broadly utilized. It has been noticed that antennas prepared for a distinct tissue are not predictable to function equally accurately, in any considerably disparate tissue around.

In this study, we suggest a clarification which covers both MICS and ISM bands for implantable purposes, as well as it can be tailored to anarbitrary tissue environment. The performance of the antenna is intensely investigated, and a spectrum of geometric variables are conferred for perfect antenna operation.

2. Materials and Methods
2.1. Antenna Design

Figure 1 illustrated the geometry of the suggested layered implantable antenna.

All dimensions of the antenna are 15x18x1.97mm³, and the antenna composed of3 copper plated substratum sheets. In this study, Roger's RO3210 as substratum was utilized since its electrical characteristic smimics with those of bio-containment substratum ceramic alumina (ε_r=9.4 and tan δ=0.006). RO3210 was favored due to its easy availability and its compatibility with ordinary manufacturing procedures making in-house prototype manufacturing possible.
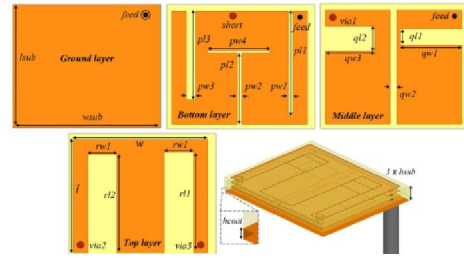

Figure 1: The geometry of suggested implantable antenna, with *lsub* = 15mm, *hsub* = 0.635mm, *wsub* = 18mm, *hcoat* = 17µm, *l* = 13.8mm and *w* = 16.56mm.

The suggested antenna composed of the ground sheet and 3 stacked patch sheets as illustrated in Figure 1. The lower layer of the antenna, supplied at the superior right corner, includes a patch with mimic slits with length and width antenna, a short pin is imported on the inferior layer as shown in Figure 1. The middle layer of the antenna includes two U-tailored paired resonators and a capacitive coupler gap [16]. The right U-tailored resonator is supplied at the superior right angle with protracted coaxial fed while the left U-tailored resonator is supplied by via1 connecting the inferior layer and the middle layer at the superior left angle, precisely opposite to the feed spot. In order to further augment the resonance efficiency of the antenna, an M-tailored, 3rdlayer is imported on the superior layer of the substratum. Via2 and via3 join the middle with the superior layer at inferior right and inferior left angles respectively. The M-tailore dupper layer contains aradiating patch with 2similar slits, with dimensions *rl1, rl2, rw1* and *rw2*respectively. λ/4 closed loop design, resonating at the principle resonant mode at 403 MHz enclose the MICS band and increased order harmonic of the similar resonant closed loop construction, was adjusted to work at 2.45 GHz ISM band. The efficacious current pathway in this antenna consists of a meandered patchon the lower layer, the left U-tailored patch of the middle layer, the M-shaped patch of the upper layer and the right U-tailored patch of the middle layer. This current pathway produces an approximately λ/4 closed loop structure, resonating at the principle resonant mode at 403 MHz inclosing the MICS band. Additionally, increased order harmonic of the similar resonant closed loop construction, was adjusted to work at 2.45 GHz ISM band, resulting in a dual band procedure using the same construction. Furthermore to increase the radiation efficacy of the suggested antenna at ISM band, the efficient length of the meandered patch on the lower layer that based upon its coupling with the ground plane was further improved.

The following step was to examine the performance of the antenna in variousnear by tissues,

which is equivalent to implanting the antenna at various body components, and to determine different antenna tuning specification concurrently, for MICS and ISM bands.

This work derive a totally parametrized antenna model with a minimal and maximal defined spectrum of geometrical limits that may optimize the efficacious wavelength of the λ/4 closed loop resonator, and the meandered patch of the lower layer.

One case is introduced in this study where the antenna is situated in 23x23x5 mm3 block of human skin phantom. Considering that the measured electrical properties of skin tissue reported in [9], were used for this procedure. As anticipated, significant detuning was noticed both at MICS and ISM bands as illustrated in Figure 2a. Results illustrated in Figure 2 (a), proved that, if the antenna was located in skin phantom, a resonant frequency shift of about 50 MHz approaching tolesser frequencies, was observed for the MICS band. Furthermore, considerable deterioration in impedance matching can be noticed in Figure 2 (a). Downshifting of the frequency was increased up to 130 MHz at the ISM band as shown in Figure 2 (b). To tune the antenna parameters on both intended frequency bands concurrently, particle swarm algorithm in addition to FDTD simulation was utilized. The outcome set of adjusted values of the antenna specifications are illustrated in the 4th column of Table 1, where the 3rd column illustrates the seed parameters for the particle swarm optimizer. The watch function to adjust the antenna in specific tissue environment is shown to be:

$$f = max(|S_{11}(dB)_{403MHz}|, |S_{11}(dB)_{2.45GHz}|)$$

It needed 20 repetitions for the particle swarm algorithm to merge and tune both minimal at the selected frequency bands. Resistance bandwidth of 9 MHz (from 398 MHz to 407 MHz) achieving the MICS band and 72 MHz (from 2438MHz to 2510 MHz) including the ISM band were accomplished due to judgment. Keeping in mind that minimal return loss can be additionally tuned at the selected frequencies at the expense of increased repetitions of the optimization algorithm. Second and third columns of Table 1 showed the range of regulating geometric specifications. The particle swarmalgorithm needs both a rang and a seed value of a geometrical specification judgement to be initiated. Parameters listed in Table 1 can be utilized for this objective. The predictable outcome must be a perfect set of parameters for which the tailored antenna works concurrently at both MICS and ISM bands and this must be, reasonable for all contributed nearby random tissue surroundings.

2.2. Methodology

The suggested implantable setup to examine over body communication composed of an implantable antenna shown in Figure 3 placed inside the stomach of a realistic high-resolution whole-body anatomical model of an adult human male phantom.

Table 1: Antenna optimization parameters in skin phantom (all values in mm)

| Parameter	min. value	max. value	seed. value	optimized
pl1	08.60	13.60	10.60	12.75
pl2	01.00	13.00	01.00	08.70
pl3	08.60	13.60	10.60	10.80
pw1	00.50	02.00	01.00	00.54
pw2	00.50	00.70	01.00	00.50
pw3	00.50	02.00	01.00	01.17
pw4	04.00	08.00	06.00	07.56
ql1	03.00	09.00	06.00	03.00
ql2	03.00	09.00	06.00	06.00
qw1	05.00	07.50	06.00	07.46
qw2	00.20	00.90	00.30	00.81
qw3	05.00	07.50	06.00	05.90
rl1	11.00	13.00	12.00	12.30
rl2	11.00	13.00	12.00	12.00
rw1	03.00	06.00	04.50	03.50
rw2	03.00	06.00	04.50	03.50

(a)

(b)
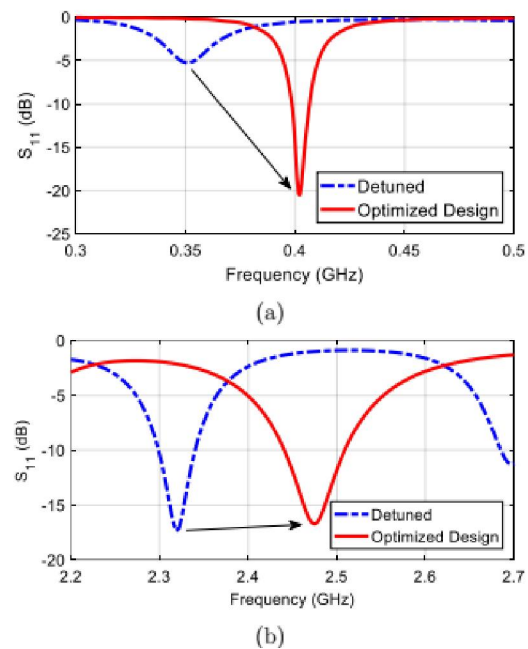
Figure 2: Detuning of antenna when placed in 23x23x5 mm human skin phantom and optimization using particle swarm algorithm at (a) MICS band and (b) ISM band
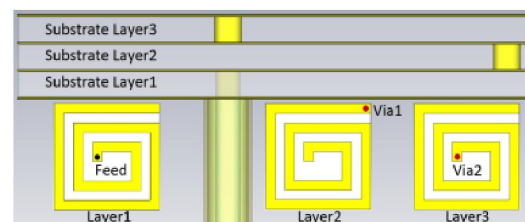

Figure 3: Geometry of implantable antenna operating at MICS band

The used antenna consists of three substrate layers of Rogers RO3210 (h=0.635mm, $\mathcal{E}_r$=9.4 and tan δ=0.006) coated with copper having spiral and meandered configuration. Three spiral layers having 1mm thick copper strip, connected to each other through via1 and via2, realize a radiating resonance at 403 MHz, MICS band. These layers are stacked to form a 3D meandered patch, in an attempt to achieve the selected denseness for an implantable antenna. The antenna utilized in this work is planned and harmonize in agreement to its procedure inside stomach of a realistic human phantom. Furthermore, a wideband antenna including directional radiation design with achieved advance varying from 4 dB to 4.5 dB at MICS band is situated beside the abdominal compartment of the phantom, to work as an outside body transceiver antenna. Preservation of the situation and work of implantable and outside body antennas fixed. Three kinds of phantoms, symbolizing human tissues have been examined as illustrated in Figure 4.

The properties of human tissues considered in this study are listed in Table 1 and were presented in [17, 15].

Note that the average human tissue properties at MICS band [89] ($\mathcal{E}_r$=35, σ =0.60 *S/m*) have been assigned to all other organs of the body phantom that are not listed in Table 2.

**Table 2: Electrical properties of human organs at MICS band**

Tissue	ϵ_r	$\sigma(S/m)$
1-Stomach	67.51	1.00
2-Abdominal Muscle	57.15	0.79
3-Body Average	35.00	0.60
4-Gallbladder	61.25	1.13
5-Large Intestine	62.63	0.95
6-Liver	51.27	0.65
7-Pancreas	61.56	0.87
8-Small Intestine	66.19	1.90
9-Spleen	63.27	1.02

As shown in Figure 4, Case1 represents a realistic human phantom model that can be considered as a reference phantom. Case2 illustrate a geometrically simpler phantom design where condensed substance blocks are situated at the same location where real human tissues are present. This layered phantom illustrates approximately simpler design than that of the realistic body phantom shown in Case1. The simplest water phantom design is illustrated in Case3 in which just those tissues which are in the LOS pathway of the implantable to outside-body antenna

communication link, are tailored for the simulation setup. These tissues are displayed by comparable substance with the implantable antenna situated interior of the corresponding stomach layer.

(a)
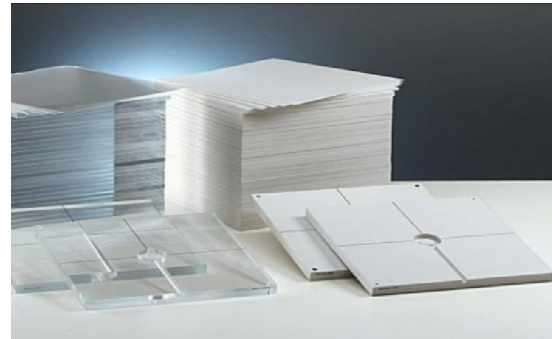
(b)

(c)

Figure 4: (a) realistic human phantom i-e Case 1; (b) complex layered phantom i-e Case 2; (c) simple water phantom i-e Case3

Thus the implantable antenna needs to be manufactured for a specific tissue medium and the variables mentioned in Table 1 should be adapted.

3. Results and Discussion

To study the performance of each phantom, Finite Difference Time-Domain (FDTD) solver with Finite Integration Perfect Boundary Approximation (FPBA) hexahedral mesh was utilized. Keeping in mind only the organs listed in Table 1, thorough wave simulation was fulfilled for all the 3 cases. The number of pulses to describe steady status concurrence characteristics was 20, and it was carefully selected to ensure accuracy up to 1%. Simulation guidelines involving adaptive mesh refinement were kept fixed for all of the 3 cases. It was noticed that a total number of FDTD mesh cells were 6.573952x106 for Case1 in comparison to that of 1.095438x106 and 0.898688x106 mesh cells accomplished in Case 2 and Case3 respectively. In Case1, the antenna is located in the stomach where it is encircled by another organs with excess water composition and significant conductivity tissues (like large intestine, and small intestine). Deliberately the antenna is harmonized with this implant as obvious by the simulated return loss shown in Figure 5.
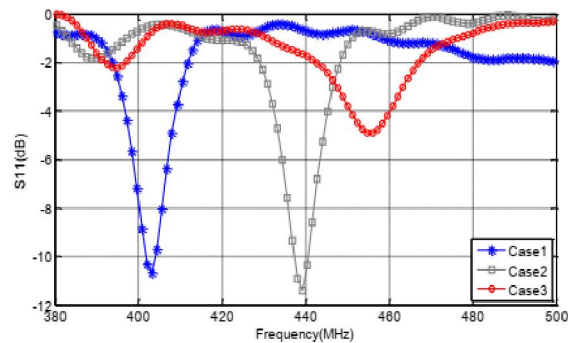

Figure 5: Return loss correlation of implantable antenna for the3 cases.

In Case2, realistic body tissues are substituted by compact substance blocks exhibiting analogously simpler designs of human tissues. Mesh cell count to simulate Case2 setup dec line however at the expense of considerable detuning of resonant frequency from 403MHz to 440 MHz. This deviation is more than the total bandwidth selected to MICS band i-e 3MHz (402 MHz-405 MHz [15]) resulting in operation of the implantable antenna outside the designated, licensed, MICS band. Moreover, when this phantom is further replaced by the second even simpler water phantom, widely used to test the performance of implantable antennas [18], the resonance frequency further shifted towards higher frequencies. S11 for Case 3 shown in Figure 6 depicts a detuning of 50 MHz, and a significant impedance mismatch.

Simulation results confirm that not only the electrical properties, but additionally the location and even the remarkable geometry of excessively conductive tissues had a prominent performance in whole-body communication. Ignoring these tissues will result in a considerable lapse in s-parameter measurement for any comparable implantable simulation setup.
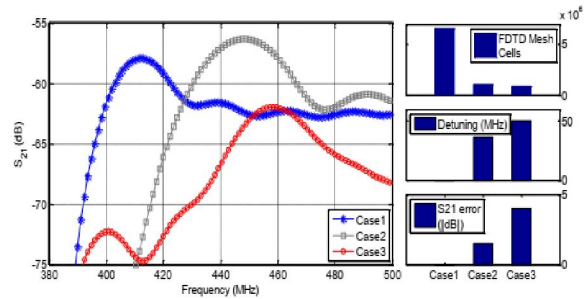

Figure 6: S21 testing for implantable antenna (left), testing of FDTD mesh cell count (Top right), testing of detuning in MHz (middle right) and testing of error noticed in S-parameter for all 3 cases.

4. Conclusions

This study describes a miniaturized implantable antenna with a meandered and stacked structure. By changing the length and width of every parameter illustrated in Table 1, the antenna is stimulated at 2 resonant frequencies, at MICS and ISM bands. It was determined that the suggested antenna can be tuned using the particle swarm algorithm, to work appropriately when situated inside multiple different human tissue models.

In this work a realistic body phantom, a complex body phantom and a widely used simple water phantom are compared in a through-body communication scenario at the MICS band. Complexity of these phantoms in terms of full wave simulator meshing density and resulting s-parameters accuracy were discussed. It was noticed that when a realistic phantom was substituted by commonly utilized simpler phantom designs, considerable detuning of the resonant frequency of the implantable antenna developed. Because of the limited bandwidth of MICS band, this detuning can be contemplated as improper for such simulation setups. More simulation outcomes determined that the added computational needs (computational means and time) to simulate a realistic body phantom modelis only 6 to 7 times the computational demands, needed to simulate simple layered phantoms or simple water phantoms. Depending on this consideration, it is favored to utilize realistic body phantom instead of layered phantoms or for simulation setups planned for implantable antennas, working in the MICS band.

References

1. E. Chow, M. Morris, and P. Irazoqui, "Implantable RF medical devices: The benefits of high- speed communication and much greater communication distances in biomedical applications," IEEE Microw. Mag., Vol. 14, No. 4: 64–73, 2013.

2. GM Aleix, C. Sergio, V. Neus, M. Jose, M. Francisco, and P. Punit, "Multilayered Broadband Antenna for Compact Embedded Implantable Medical Devices: Design and Characterization," Progress In Electromagnetics Research, Vol. 159: 1–13, 2017.

3. J. Gemio, J. Parron, and J. Soler, "Human body effects on implantableantennas for ism bands applications: Models comparison and propagationlosses study," Progress in Electromagnetics Research, vol. 110, pp. 437- 452,2010.

4. H. Permana, Q. Fang, and W. S. Rowe, "Hermetic implantable antennainside vitreous humor simulating fluid," Progress In Electromagnetics Research, vol. 133: pp. 571 - 590, 2013.

5. T. Yilmaz, R. Foster, and Y. Hao, "Patch resonator for non-invasive detection of dielectric property changes in biological tissues," in Antennasand Propagation Society International Symposium (APSURSI), 2012 IEEE, pp. 1- 2, IEEE, 2012.

6. R. Alrawashdeh, Y. Huang, and P. Cao, "Flexible meandered loop antennafor implants in medradio and ism bands," Electronics Letters, vol. 49, no. 24: pp. 1515- 1517, 2013.

7. T. Karacolak, R. Cooper, and E. Topsakal, "Electrical properties of rat skinand design of implantable antennas for medical wireless telemetry," IEEE Transactions on Antennas and Propagation, vol. 57, no. 9: pp. 2806- 2812,2009.

8. Z. Noroozi and F. Hojjat-Kashani, "Three-dimensional fdtd analysis ofthe dual-band implantable antenna for continuous glucose monitoring," Progress In Electromagnetics Research Letters, vol. 28: pp. 9- 21, 2012.

9. T. Karacolak, R. Cooper, J. Butler, S. Fisher, and E. Topsakal, "In vivoverification of implantable antennas using rats as model animals," IEEEAntennas and Wireless Propagation Letters, vol. 9: pp. 334- 337, 2010.

10. F. Merli, L. Bolomey, J.-F. Zurcher, G. Corradini, E. Meurville, and A. K. Skrivervik, "Design, realization and measurements of a miniature antennafor implantable wireless communication systems," IEEE Transactions on Antennas and Propagation, vol. 59, no. 10: pp. 3544- 3555, 2011.

11. J. Kim and Y. Rahmat-Samii, "Planar inverted-f antennas on implantablemedical devices: Meandered type versus spiral type," Microwave and Optical Technology Letters, vol. 48, no. 3: pp. 567- 572, 2006.

12. N. Vidal, S. Curto, J. M. Lopez-Villegas, J. Sieiro, and F. M. Ramos,"Detuning study of implantable antennas inside the human body," Progress In Electromagnetics Research, vol. 124: pp. 265- 283, 2012.

13. J. Abadia, F. Merli, J.-F. Zurcher, J. R. Mosig, and A. K. Skrivervik, "3dspiral small antenna design and realization for biomedical telemetry in themics band," Radioengineering, vol. 18, no. 4: pp. 359- 367, 2009.

14. F.-J. Huang, C.-M. Lee, C.-L. Chang, L.-K. Chen, T.-C. Yo, and C.-H. Luo, "Rectenna application of miniaturized implantable antenna design for triple-band biotelemetry communication," IEEE Transactions on Antennasand Propagation, vol. 59, no. 7: pp. 2646- 2653, 2011.

15. A. Kiourti and K. S. Nikita, "A review of implantable patch antennas forbiomedical telemetry: Challenges and solutions [wireless corner]," IEEEAntennas and Propagation Magazine, vol. 54, no. 3: pp. 210- 228, 2012.

16. M. Abbasi, S. Shahid, M. Rizwan, M. Tarar, and S. Abbas, "On-boardprinted handset antenna with coupled monopoles," in Antennas and Propagation (EuCAP), 20148th European Conference on, pp. 2889- 2892, IEEE,2014.

17. A. Sani, A. Alomainy, and Y. Hao, "Numerical characterization of the radiation from implanted wireless sources considering different digital bodyphantoms," in Antennas and Propagation, 2009. EuCAP 2009, 3rd European Conference on: pp. 459- 461, IEEE, 2009.

18. S.-M. Huang, M.-R. Tofighi, and A. Rosen, "Considerations for the design and placement of implantable annular slot antennas for intracranialpressure monitoring devices," IEEE Antennas and Wireless Propagation Letters, vol. 14: pp. 1514- 1517, 2015.

19. Baidu. http://www.baidu.com. 2019.

20. Google. http://www.google.com. 2019.

21. Journal of American Science. http://www.jofamericanscience.org. 2019.

22. Life Science Journal. http://www.lifesciencesite.com. 2019.

23. Ma H, Cherng S. Nature of Life. Life Science Journal 2005;2(1):7-15. doi:10.7537/marslsj020105.03. http://www.lifesciencesite.com/lsj/life0201/life-0201-03.pdf.

24. Ma H. The Nature of Time and Space. Nature and science 2003;1(1):1-11. doi:10.7537/marsnsj010103.01. http://www.sciencepub.net/nature/0101/01-ma.pdf.
25. Marsland Press. http://www.sciencepub.net. 2019; http://www.sciencepub.org. 2019.
26. National Center for Biotechnology Information, U.S. National Library of Medicine. http://www.ncbi.nlm.nih.gov/pubmed. 2019.
27. Nature and Science. http://www.sciencepub.net/nature. 2019.
28. Stem Cell. http://www.sciencepub.net/stem. 2019.
29. Wikipedia. The free encyclopedia. http://en.wikipedia.org. 2019.

5/4/2019